

Direct growth of III-V laser structures on silicon substrates

From infrared to ultraviolet wavelengths, researchers are enabling lower-cost production of silicon photonics. **Mike Cooke** reports.

The components of a silicon photonics platform integrating optical communications and silicon electronics are coming together. Among the aims of various research groups are the future development of co-integrated CMOS-compatible optical data links and data processing electronics. End applications include biological sensing, cloud-based applications, 'big-data' services and enterprise data centers.

The most difficult part of the equation is creating suitable light sources: efficient laser diodes (LDs) and other light-emitting devices are challenging on silicon photonics platforms since they require direct-bandgap semiconductors, in contrast to the indirect bandgap of silicon.

Growing advanced light-emitting III-V semiconductors on silicon suffers from challenges arising from lattice mismatches, thermal mismatches and charge polarity mismatches, generation of antiphase boundaries, etc. There are techniques to mitigate many of these problems, such as off-axis substrates to combat anti-phase boundaries, but they come at the cost of reduced compatibility with silicon microelectronics fabrication/integration and increased production expense.

Instead, such integration is often achieved using wafer bonding of separate III-V and silicon structures. However, monolithic growth would be preferred since it is expected to result in low-cost, high-yield and large-

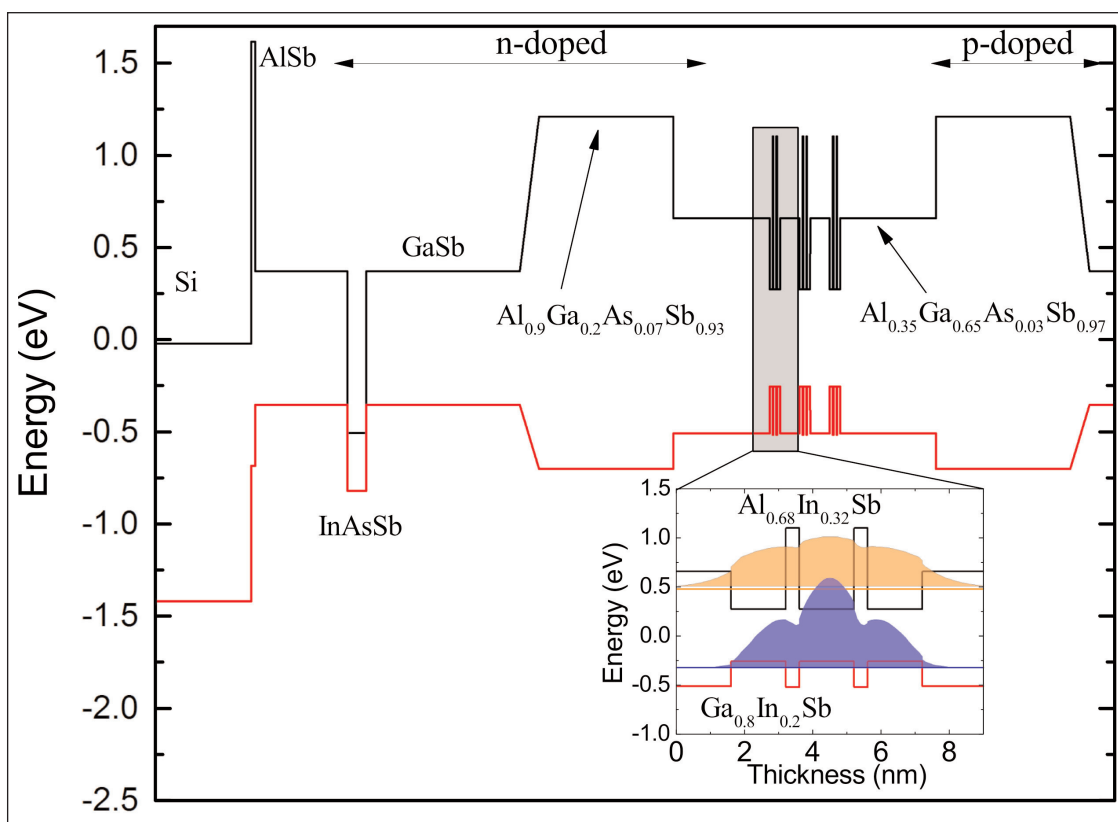


Figure 1. Simulated bandstructure of whole GaSb-on-Si laser heterostructure. Inset: GaInSb/AlInSb composite quantum well details with confined electron and hole levels and wavefunctions.

scale integration of complex optoelectronic circuits. Here we look at recent progress in monolithic direct growth of III-V semiconductors on silicon.

Fiber-optic gallium antimonide

Université de Montpellier and III-V Lab in France have developed monolithic quaternary aluminium gallium arsenide antimonide (AlGaAsSb) growth on silicon, producing laser diodes emitting at close to the 1.55 μm optimum wavelength for fiber-optic telecommunications [A. Castellano et al, APL Photonics, vol2, p061301, 2017]. Normally, GaSb-based laser diodes operate best in the mid-infrared range (longer than 3 μm).

While there has been progress with devices emitting at

wavelengths away from 1.55 μm , previous work of the researchers struggled to create laser diodes at 1.55 μm — “these lasers suffered from high threshold current densities, resulting in poor performances limited to pulsed operation,” the team writes.

The latest laser material was produced using molecular beam epitaxy (MBE) on quarters of 2-inch (001) silicon wafers that were offcut 6° in the [110] direction. The offcut angle was designed to restrict formation of anti-phase domains arising from charge polarity differences in the chemical bonds between the substrate and III-V compound semiconductors.

The growth was nucleated with 4 monolayers of 450°C AlSb. The researchers then grew 1 μm of GaSb while ramping up to 500°C, 150nm of lattice-matched indium arsenide antimonide (InAs_{0.92}Sb_{0.08}) etch stop/n-contact, and 800nm of 470°C n-GaSb.

The rest of the structure was grown at 470°C and consisted of 1.5 μm of doped Al_{0.9}Ga_{0.1}As_{0.07}Sb_{0.93} cladding and 230nm of undoped Al_{0.35}Ga_{0.65}As_{0.03}Sb_{0.97} waveguide layers above and below the active light-emitting quantum wells. Graded AlGaAsSb layers were used to smooth the band profiles between the buffer and n-cladding, and between the p-cladding and p-GaSb contact layer (Figure 1). Beryllium and tellurium were used for the p- and n-type doping, respectively.

The active region consisted of three Ga_{0.80}In_{0.20}Sb/Al_{0.68}In_{0.32}Sb quantum wells separated by 20nm of Al_{0.35}Ga_{0.65}As_{0.03}Sb_{0.97} barriers. The composite well contained 6nm of GaInSb with two insertions of 0.45nm AlInSb. The strain is estimated at 1.35% relative to the GaSb lattice. The wells have a ‘type-I’ structure where electron and hole wavefunctions overlap by 96.2%, according to simulations. High overlap should lead to better recombination into photons.

The researchers comment: “The confined electron and hole levels are located 180meV and 190meV below the barrier level, respectively (Figure 1). Although sufficient for the holes, this confinement energy is not high enough to totally suppress thermal escape of electrons out of the QWs at room temperature and above.”

The laser diodes were fabricated in a ridge format with gold-germanium-nickel alloy n-contacts on either side of the ridge and titanium-gold p-contact on top of the ridge. Electrical insulation was provided by photoresist material. The n-contact with the InAsSb layer avoids current flow through the highly defective GaSb buffer region near the silicon substrate, improving performance.

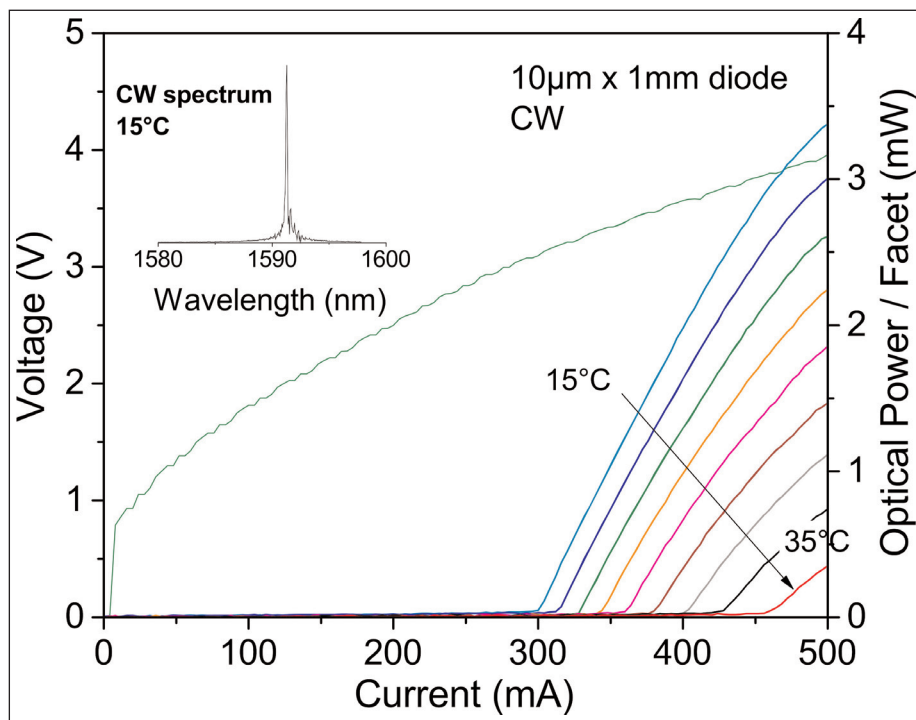


Figure 2. Light output power and voltage versus current curves from 10 μm x 1mm narrow-ridge laser diode under cw operation between 15°C and 35°C. Inset: laser emission spectrum at 15°C.

Mirror facets for the laser cavity were obtained by simple cleaving with no optical treatment to increase reflectivity. The devices were mounted epi-side up on copper heat-sinks.

Room-temperature pulsed operation of 100 μm x 1mm broad-ridge laser diodes gave a threshold current density of 1kA/cm² — a value comparable with devices produced on GaSb substrate, according to the researchers. The series resistance was 3 Ω and the turn-on voltage was 0.8V, close to the value expected from the bandgap.

Continuous wave (cw) current injection in 10 μm x 1mm narrow-ridge laser diodes result in threshold currents of 300mA at 15°C and 450mA at 35°C, corresponding to a T_0 characteristic temperature of 50K (Figure 2). The researchers claim that this is comparable to what is seen in 2 μm -wavelength GaSb lasers on silicon and to initial InP-based quantum well devices grown on indium phosphide (InP) emitting near 1.55 μm with comparable carrier confinement. At 500mA injection, the narrow-ridge laser diodes output 3.5mW at 15°C and 3mW at 35°C. Higher power could be achieved by increasing current injection towards thermal roll-over. Treating the facets to improve the laser cavity could also boost performance.

At a temperature of 15°C, the laser wavelength was 1.59 μm , which corresponds to the C/L bands (1530–1565nm/1565–1625nm) for high-performance optical telecoms. [The C-band corresponds to the lowest-attenuation fiber for dense wavelength-division multiplexing (DWDM). L-band also has low attenuation and allows the use of DWDM.]

► The variation in performance was represented by a threshold current density that ranges between 1 kA/cm^2 and 1.5 kA/cm^2 for the broad-ridge devices at room temperature. The narrow-ridge laser diodes had thresholds between 300mA and 500mA. The researchers comment: "At this stage, we ascribe these variations to different facet qualities of the laser diodes. Indeed, silicon does not spontaneously cleave along the [110] crystal direction as the III-V semiconductors do to form natural facets."

1.55 μm quantum dot lasers

Hong Kong University of Science and Technology (HKUST) and Harvard University in the USA have reported progress on direct epitaxy of III-V quantum dot (QD) materials on silicon, producing 1.55 μm -wavelength microdisk lasers (MDLs) [Bei Shi et al, Appl. Phys. Lett., vol110, p121109, 2017]. Normally, 1.55 μm III-V devices are grown on InP. Electrically driven III-V quantum dot laser materials on silicon have recently been realized for shorter, non-optimal

1.3 μm optical fiber wavelengths. The HKUST/Harvard team sees their work as "a promising path towards large-scale integration of cost-effective and energy-efficient silicon-based long-wavelength lasers."

Quantum dots are seen as a way to lower laser thresholds, to improve thermal stability, and to increase robustness against the effects of defects.

The III-V material was all grown on (001) silicon using metal-organic chemical vapor deposition (MOCVD). A number of strategies were deployed to reduce threading dislocations, anti-phase boundaries, and other common defects arising from the 8% mismatch between the InP and silicon crystal lattices (Figure 3):

1. A 1.7 μm -thick GaAs intermediate buffer to accommodate the InP/Si mismatch. The GaAs buffer incorporated an AlGaAs/GaAs strained-layer superlattice (SLS) to reduce dislocation densities and give a smooth surface.
2. The InP buffer layer was grown in stages, starting with a 70nm low-temperature nucleation and continuing with 1.4 μm of InP buffer grown in multiple temperature

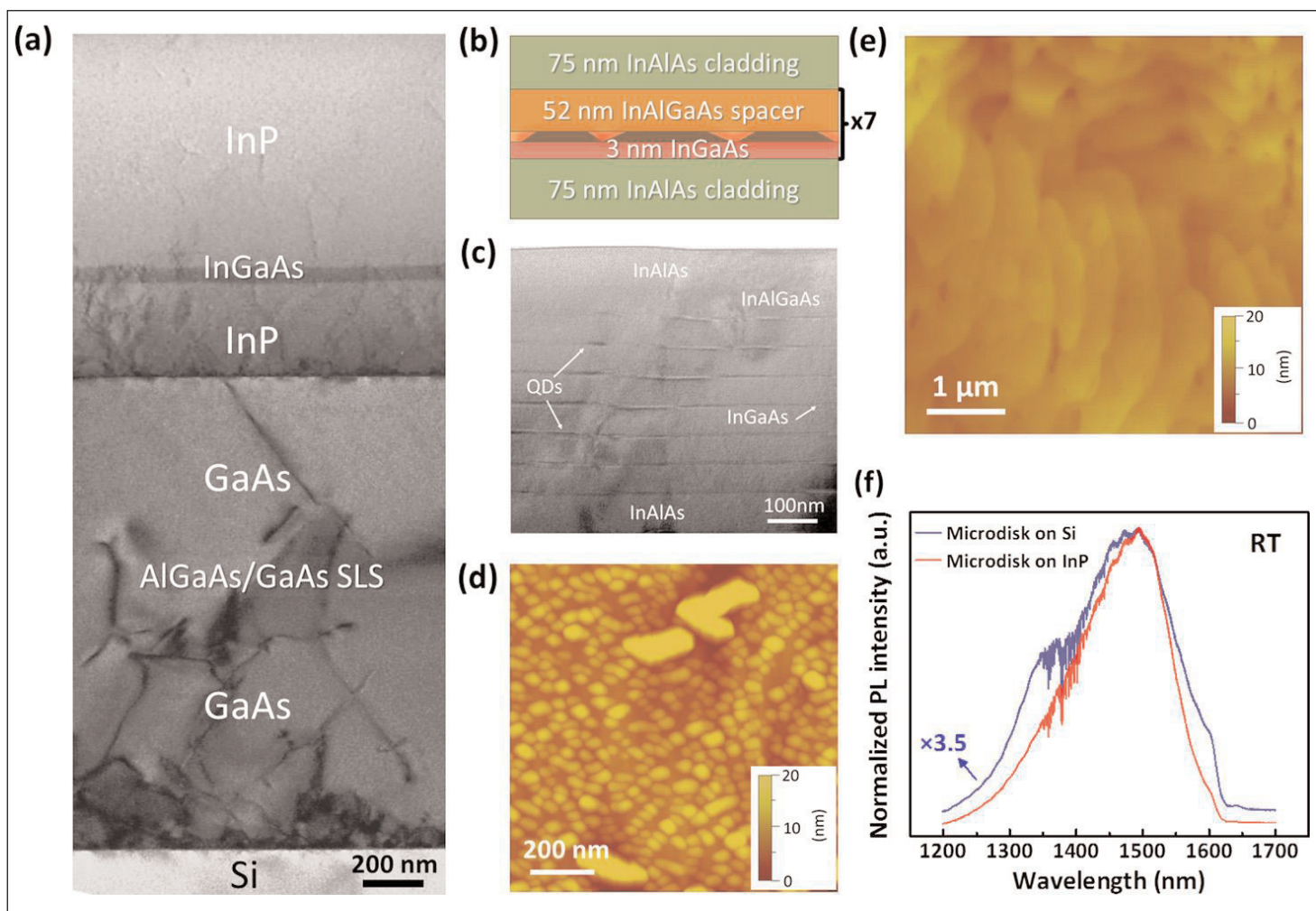


Figure 3. (a) Cross-sectional transmission electron microscope (TEM) image of InP/Si template; (b) schematic of microdisk laser structure; (c) close-up TEM of the microdisk laser on silicon, highlighting InAlAs/InGaAs/InAlGaAs DWELLS; (d) representative surface morphology of uncapped InAs QDs on top of InP/Si substrate; (e) typical $5\mu\text{m} \times 5\mu\text{m}$ atomic force microscope image of InP thin-film surface grown on Si; (f) room-temperature photoluminescence of as-grown microdisk laser material on Si and InP substrates, respectively.

steps. The InP buffer included a 60nm $\text{In}_{0.6}\text{Ga}_{0.4}\text{As}$ strained-interlayer designed to filter dislocations from the GaAs/InP interface.

The resulting InP/Si template surface had 1.6nm root-mean-square roughness, according to $5\mu\text{m} \times 5\mu\text{m}$ atomic force microscopy.

The microdisk laser structure consisted of a 7-period quantum dot in well (DWELL) structure sandwiched between 75nm InAlAs cladding layers. The InAs quantum dots had a typical diameter of 45nm with $4 \times 10^{10}/\text{cm}^2$ density. The 3nm-thick InGaAs served as a wetting layer. The InAlGaAs was applied in two steps: 1.5nm low-temperature material to avoid desorption of the underlying dots, and a 52nm high-temperature spacer layer. The high temperature also annealed the dots to prevent dot-height dispersion and to tune the emission wavelength.

Comparing the photoluminescence (PL) with material grown on InP substrates showed a factor of 3.5 lower emission from the structure grown on the InP/Si template. The emission line was broader and a shoulder was present in the latter material. The researchers suggest that this could be due to dot-size fluctuation. They add: "The broad spectra however favor the interaction between resonant modes in small cavities and the material gain."

Lasers consisted of $1.5\mu\text{m}$ -diameter microdisks formed by colloidal lithography and dry etching down to the InP buffer. A selective wet etch then formed an InP pillar.

The laser was pumped using a 532nm Q-switched neodymium-doped yttrium aluminium garnet (Nd:YAG) pulsed laser source (20ns pulse width, 3000Hz repetition rate). Stimulated emission with a 1563nm wavelength was achieved with a high background suppression ratio of 21.7dB. There was some increase in line-width above threshold, attributed to wavelength chirping from changes in refractive index caused by transient changes of carrier density in the QDs.

The threshold pumping power was $2.73 \pm 0.23\text{mW}$. The researchers say this is an upper bound, since no account was taken of multiple reflection/absorptions inside the disk and coupling efficiency of the pump beam.

Statistical studies with various $1.5\mu\text{m}$ and $4\mu\text{m}$ disk diameters demonstrated thresholds for devices on InP/Si templates about twice that of lasers produced on pure InP substrates (Figure 4). The team comments: "The larger thresholds on silicon are mainly associated with three factors. First, the material gain in the QD active region on silicon is somewhat lower due to non-radiative recombination processes introduced by crystalline defects. Second, the injection efficiency is reduced because the pump-laser-generated carriers can be partially trapped by the deep energy level traps related with dislocations in the disk region. Moreover, the broader PL emission spectrum of the MDL on silicon is more favorable for multi-mode lasers."

Varying the temperature up to 60°C , the researchers extracted a high threshold characteristic (T_0) of 123K

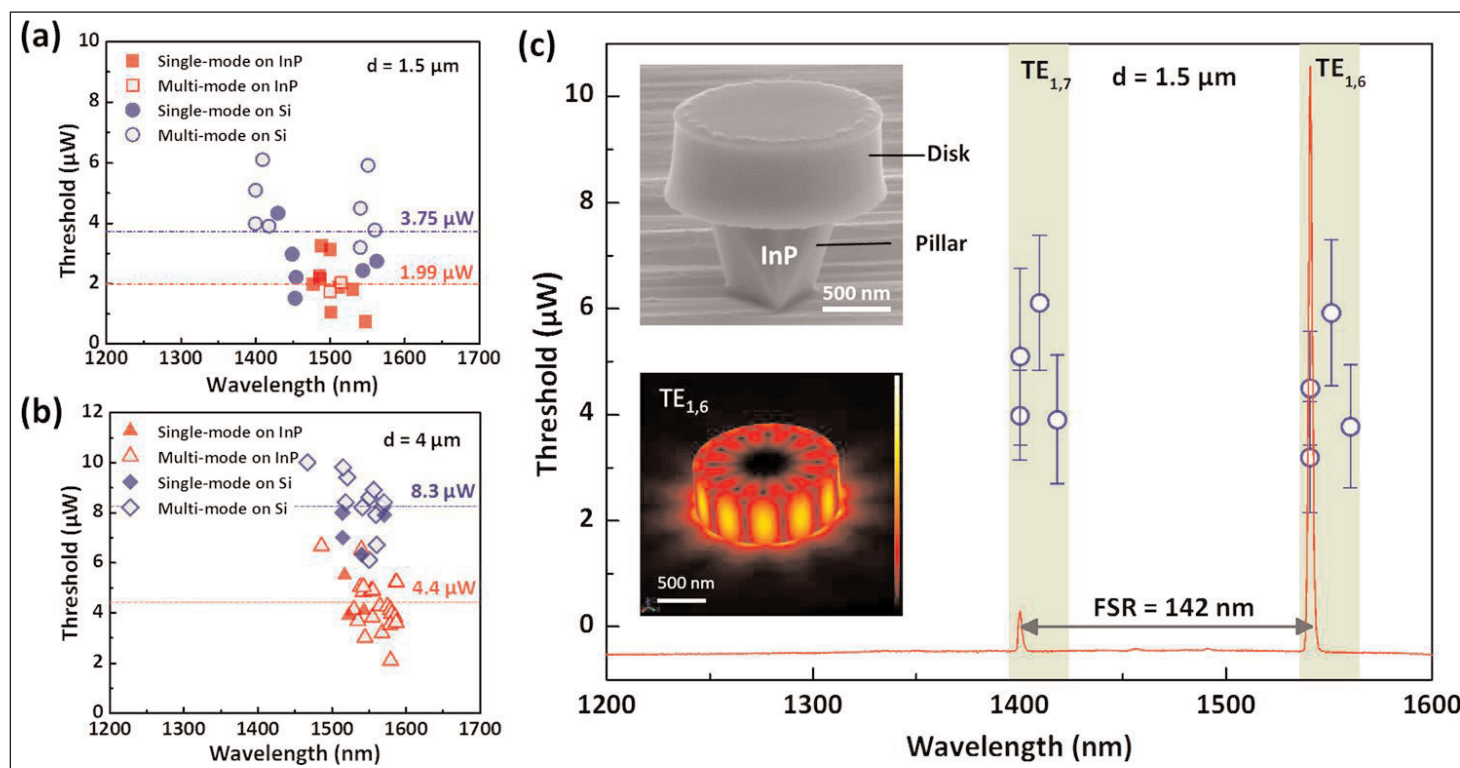


Figure 4. Single-mode (solid symbols) and multi-mode (open symbols) lasing threshold dispersion of (a) $1.5\mu\text{m}$ and (b) $4\mu\text{m}$ microdisks on InP and Si as function of wavelength. (c) Overlay of threshold powers in multi-mode $1.5\mu\text{m}$ disks with representative lasing spectrum. Top inset: scanning electron microscope image; bottom inset: three-dimensional electric field distribution of simulated $\text{TE}_{1,6}$ mode.

for one mode ($TE_{1,6}$, 1546.9nm). They describe this value as “among the best reported T_0 for QD MDLs on III-V substrates.” The other mode studied ($TE_{1,7}$, 1406.2nm) had a lower T_0 of 90K. The team comments: “the larger T_0 of the $TE_{1,6}$ mode can be attributed to a better overlap with the gain spectrum at higher temperatures and a superior carrier capture efficiency in larger QDs, which prevent carrier evaporation into barriers.”

Electrical pumping of InAs QDs

University College London in the UK and Univ. Grenoble Alpes in France have claimed the first electrically pumped cw InAs in GaAs quantum dot (QD) lasers directly grown on industry-compatible nominal silicon (001) substrates without any intermediate buffers [Siming Chen et al, Optics Express, vol25, p4632, 2017]. The team used a combination of MOCVD and MBE on microelectronics standard on-axis Si (001) 300mm diameter wafers. The MOCVD stage involved an Applied Materials tool.

The silicon surface was prepared by cleaning and annealing at 900°C in hydrogen to reconstruct the surface structure to promote GaAs quality. After the anneal, the temperature was reduced to 700°C in 30 seconds to ‘freeze’ in the surface reconstruction.

A two-step MOCVD was carried out to give a 40nm 400–500°C GaAs layer and a 360nm 600–700°C GaAs layer. The researchers say that the 400nm GaAs layer on silicon was antiphase-boundary free.

The MBE for the QD laser structure (Figure 5) was carried out in a 3-inch Veeco tool, so the virtual GaAs/Si substrate material had to be diced down to fit into the reaction chamber. The epitaxial design included n-InGaAs/GaAs strained-layer superlattices (SLSs) aiming at blocking threading dislocations from entering the active region. The cladding layers were $Al_{0.4}Ga_{0.6}As$, while the 30nm waveguide regions above and below the active region were $Al_{0.12}Ga_{0.88}As$.

The ‘dot-in-well’ (DWELL) active region consisted of five sequences of InAs/InGaAs/GaAs dot

regions separated by 50nm GaAs spacers. The dot density of uncapped layers was around $3.5 \times 10^{10}/cm^2$, according to atomic force microscopy. This compares with $3 \times 10^{10}/cm^2$ for dots grown on GaAs substrates.

The material was used to fabricate broad-area lasers. Mesa structures were wet etched down to about 100nm above the active region. Further etching reached down to the n-GaAs buffer layer. Titanium/platinum/gold and nickel/germanium/gold/nickel/gold were used for the p- and n-electrodes, respectively. The silicon substrate was thinned to 120mm before cleaving into laser bars.

Testing was carried out on 3mm-long 25µm-wide devices mounted on copper heat-sinks. Gold wire-bonding was used for electrical connections. The facets were uncoated.

While the series resistance of devices on GaAs/Si and pure GaAs were similar, the QD laser performance was degraded for GaAs/Si compared with pure GaAs substrates. In particular, the threshold current density increased from 210A/cm² to 425A/cm² (Figure 6). Also, the slope efficiency of the laser on GaAs/Si was reduced to 0.068W/A, compared with 0.12W/A for pure GaAs-based devices. The external quantum differential efficiencies were 7.2% and 12.7% for GaAs/Si and pure GaAs, respectively.

The researchers comment: “Compared with the laser device grown on native GaAs substrate, the degraded device performances for QD laser grown on the Si (001) substrate is related to the defects propagating into the QD active layers.”

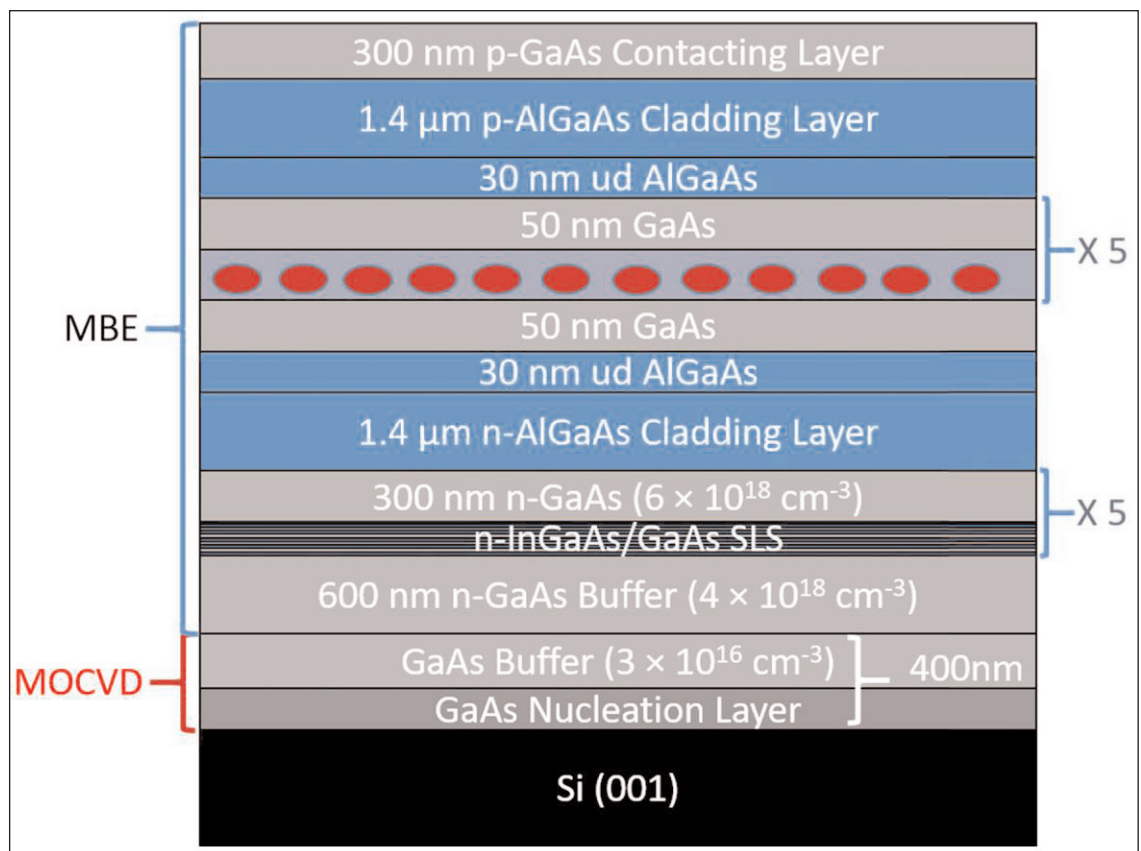


Figure 5. Schematic of QD laser structure grown on on-axis Si (001) substrate.

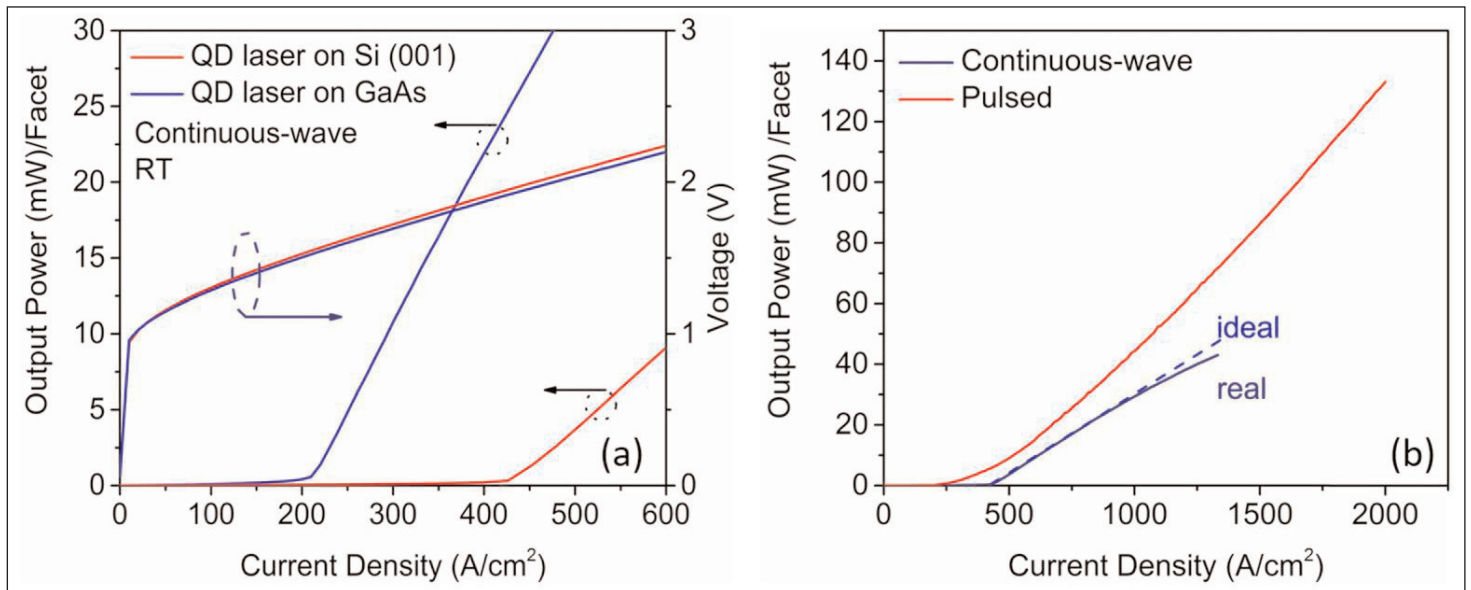


Figure 6. (a) Power-current-voltage (LIV) characteristics comparison of InAs/GaAs QD laser grown on GaAs/Si (001) to reference QD laser grown on native GaAs substrate at room temperature under cw operation. (b) LI comparison of InAs/GaAs QD laser grown on GaAs/Si (001) substrate under cw and pulsed operation conditions at room temperature.

The maximum single-facet output power of the QD laser on GaAs/Si was 43mW at 1332A/cm² cw injection. Pulsed operation increased the maximum to 134mW at 2kA/cm² injection.

The cw spectrum of the QD laser on GaAs/Si had a peak at 1292nm (1.3μm) with 49nm full-width half-maximum (FWHM) at a subthreshold current density of 267A/cm². Above threshold the FWHM narrowed to around 2.2nm. At higher current, the spectral output showed multiple peaks (i.e. multi-mode behavior).

Temperature-dependent pulse-mode operation saw lasing operation up to 102°C. "To the best of knowledge, this is the first demonstration of QD lasers monolithically grown on exact silicon (001) substrate that lase over to 100°C," the team writes. The maximum temperature for cw lasing was 36°C.

The team points out that the performance is also down on QD lasers grown on off-cut silicon wafers. Further optimization should be possible. The researchers comment: "Nevertheless, good cw performance has been achieved, and the threshold current density reported in the present work has been reduced by more than a factor of two, compared with the very recent achievement of an InAs/GaAs QD laser on on-axis Si (001) substrate with an intermediate GaP buffer layer."

Visible and ultraviolet III-nitride

Researchers in France have created a range of optically pumped III-nitride microdisk lasers on silicon covering a wide range of wavelengths, from 280nm deep ultraviolet to 500nm blue-green/cyan [J. Sellés, Appl. Phys. Lett., vol109, p231101, 2016]. Two types of multiple quantum well structure were produced: gallium nitride (GaN) wells with aluminium nitride (AlN) barriers

(deep UV), and indium gallium nitride (InGaN) with gallium nitride barriers (violet and blue-green).

The non-alloyed GaN/AlN structures avoid spectral broadening from alloy disorder, compared with more usual AlGaIn-based samples. Further, "low interface roughness limits the impact of monolayer fluctuations on the QW transition energy," according to the team.

The team from Laboratoire Charles Coulomb, Centre de Nanosciences et de Nanotechnologies, Centre de Recherche pour l'Hétéro-Epitaxie et ses Applications, Université Grenoble Alpes, and Institut Nanosciences et Cryogénie (INAC), see their work as complementary to the development of infrared integrated photonics for telecommunications. In the case of visible-UV devices, potential applications include bio-chemical analysis and on-chip optical interconnects.

The researchers add: "The broad tunability paves the way to the development of a UV-visible integrated photonic platform embedding microlasers, possibly addressing multiple wavelengths. A further step will deal with the electrical injection, following the recent progresses in electrically injected InGaN lasers on Si-substrates."

Ammonia MBE was used on (111)-oriented silicon to produce a range of GaN/AlN and InGaN/GaN structures (Table 1). All the structures were grown on an AlN buffer. The InGaN/GaN structures also included a GaN buffer on top of the AlN. In the InGaN-2 sample, the GaN buffer was silicon-doped to encourage electron injection into the multiple quantum well active region.

Microdisks were patterned and dry etched before selective under-etch of the substrate to create microdisks (3μm to 12μm diameter) on silicon pedestals (Figure 7). The output was derived from

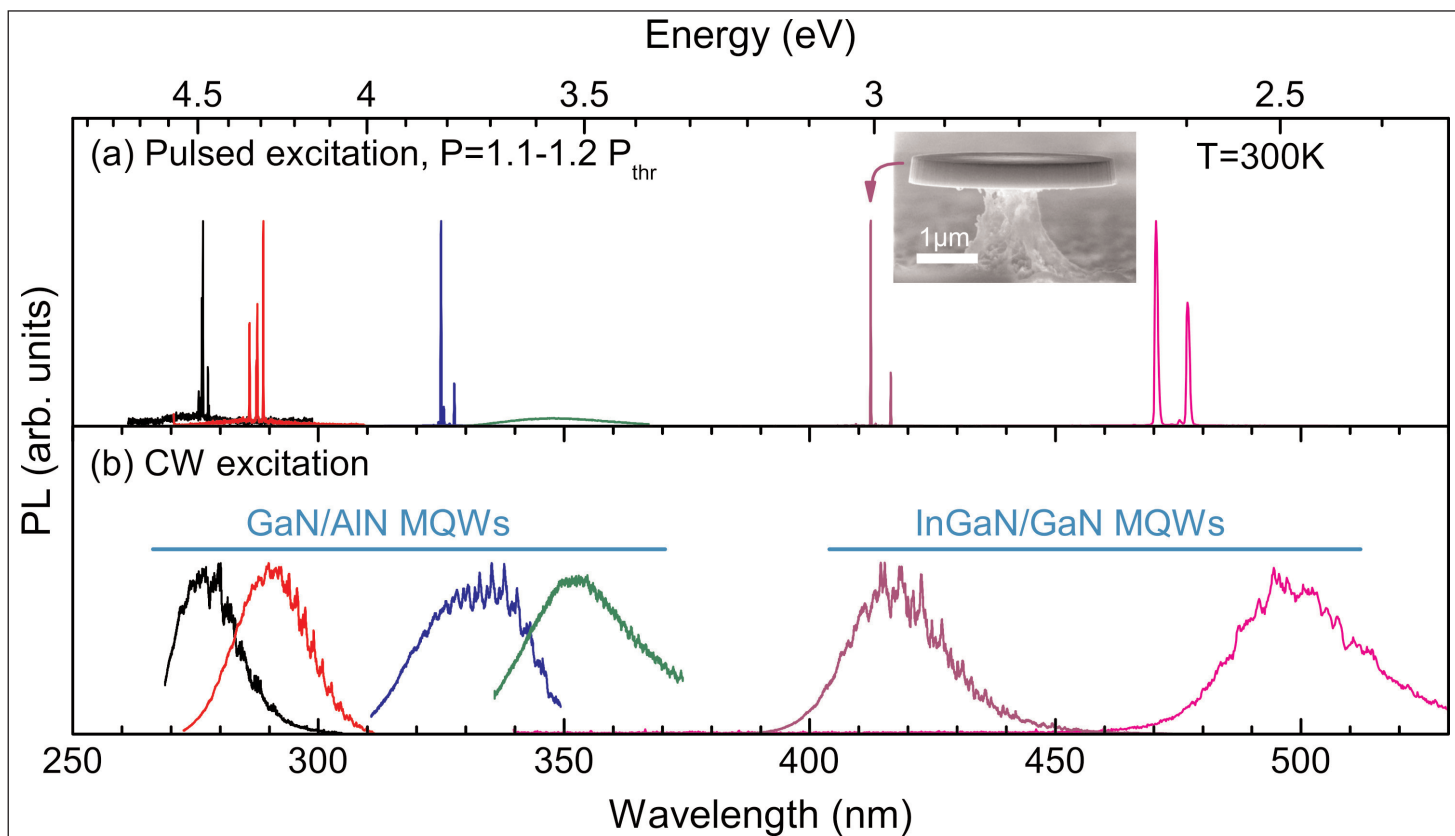


Figure 7. Photoluminescence spectra of 6 microdisk samples (from left to right, GaN-1 to GaN-4, InGaN-1, InGaN-2); (a) microlaser spectrum above threshold, under pulsed optical pumping; (b) microdisk spectrum in linear regime, under cw excitation. Inset electron micrograph of 4 μ m microdisk from InGaN-1 series.

Table 1. Sample active layers.

Sample	Well/barrier materials	Well thickness (nm)	Number	cw wavelength (nm)
GaN-1	GaN/AlN	0.7	20	280
GaN-2	GaN/AlN	0.7	10	290
GaN-3	GaN/AlN	1.2	10	330
GaN-4	GaN/AlN	1.8	10	350
InGaN-1	In _{0.12} Ga _{0.88} N/GaN	2.2	10	417
InGaN-2	In _{0.2} Ga _{0.8} N/GaN	2.2	10	500

Table 2. Microdisk geometries and microlaser characteristics.

Sample	Resonator			Laser	
	Diameter (μ m)	Thickness (nm)	Q	Threshold (mJ-cm ² /pulse)	Wavelength (nm)
GaN-1	3	220	4000	15	275
GaN-2	6	160	2000	27	290
GaN-3	6	160	2000	35	330
GaN-4	6	160	>1000		
InGaN-1	4	515	2500	3	412
InGaN-2	5	1300	2500	3	47

optical pumping with 266nm-wavelength laser light with cw or pulsed (400ps, 4kHz) operation. The longest-wavelength GaN-4 device was unable to achieve lasing — the researchers attribute this to the quantum-confined Stark effect, where electric fields

from charge polarization of the III-nitride bonds inhibit electron-hole recombination into photons. GaN-4 contains the thickest wells, compared to the other devices.

The laser threshold was an order of magnitude smaller for the InGaN/GaN devices, compared with GaN/AlN microdisks (Table 2). "This can be interpreted as the difference between resonant and non-resonant excitation," the researchers write. "Indeed, the laser energy is below the AlN bandgap and above the GaN bandgap. The 266nm laser pumps the excited states of the GaN/AlN QW, and the 10 QWs can only absorb part of it. On the contrary, the entire pulse energy is absorbed by the GaN barrier in the case of InGaN

QWs, leading to a larger carrier density per QW if we assume that all carriers are transferred from the barrier to the well." ■

Author: Mike Cooke